Configuration Control Studies of Heliotron J

F.Sano 1), T.Mizuuchi 1), K.Kondo 2), K.Nagasaki 1), H.Okada 1), S.Kobayashi 1), K.Hanatani 1), Y.Nakamura 2), Y.Torii 3), S.Yamamoto 4), M.Yokoyama 5), Y. Suzuki 5), M.Kaneko 2), H.Arimoto 2), G.Motojima 2), S.Fujikawa 2), H.Kitagawa 2), H. Nakamura 2), T.Tsuji 2), M.Uno 2), H.Yabutani 2), S.Watanabe 2), S.Matsuoka 2), M.Nosaku 2), N.Watanabe 2), T.Tomokiyo 2), N.Nishino 6), Z.Feng 7), Y.Ijiri 1), T.Senju 1), K. Yaguchi 1), K. Sakamoto 1), K. Tohshi 1), M.Shibano 1)

1) Institute of Advanced Energy, Kyoto University, Gokasho, Uji, Japan, 2) Graduate School of Energy Science, Kyoto University, Kyoto, Japan, 3) High Temperature Plasma Center, University of Tokyo, Chiba, Japan, 4) Graduate School of Engineering, Osaka University, Suita, Japan, 5) National Institute for Fusion Science, Gifu, Toki, Japan, 6) Graduate School of Engineering, Hiroshima University, Hiroshima, Japan, 7) Southwestern Institute of Physics, Chengdu, China

e-mail contact of main author: sano@iae.kyoto-u.ac.jp

Abstract. Configuration control studies of Heliotron J (a low shear helical-axis heliotron having 4 periods, $\iota(a)/2\pi$ = 0.3-0.8, R~1.2 m, a=0.1~0.2 m and $B_o \leq 1.5$ T) have been carried out with an emphasis on the confinement improvement by the bumpy field which should play a key role in the neoclassical optimization of the helical-axis heliotron. Measurements of the enhancement factor (H_{ISS04}) of the experimental global energy confinement time (τ_E^{exp}) with regard to the recent international stellarator scaling law (τ_E^{ISS04}) have been made for 0.3-MW, 70-GHz on-axis ECH plasmas by changing the bumpiness (ε_b) under the basically similar average magnetic axis position (R_{ax}), minor plasma radius (a) and edge rotational transform ($\iota(a)/2\pi$) conditions. The experimental analysis suggests that the reduction of the "effective helical ripple", ε_{eff}, may introduce a beneficial effect on the improvement of H_{ISS04} not only in the L-mode but also in the transient phase of the H-mode. The related bumpiness modification studies are also discussed.

1. Introduction

The confinement studies of Heliotron J in these two years have focused on five important topics of the configuration control studies of low-β helical-axis heliotron plasmas based on the edge rotational transform ($\iota(a)/2\pi$) control and the bumpiness (ε_b) control with regard to: (i) thermal confinement, (ii) fast ion confinement, (iii) bootstrap and electron cyclotron (EC) driven current control, (iv) edge/SOL plasma properties and (v) divertor plasma dynamics. This paper presents the new experimental results obtained after the previous 20th IAEA Conference [1] with special reference to thermal confinement and related studies. The companion papers in this conference deal with other topics related to the ion cyclotron range of frequency (ICRF) heating [2], bootstrap and EC driven currents [3] and divertor plasma dynamics [4].

One of the objectives of the confinement studies of Heliotron J is to extend the understanding of neoclassical transport of the 3-D plasmas and the related role of configuration parameters such as bumpiness in transport reduction and/or toroidal current control of the omnigeneous optimization scenario of a helical-axis heliotron. Although there are dimensional constraints that follow from invariance principles, studying plasma transport in terms of the non-dimensional field geometry parameters (R/a, $\iota/2\pi$, $\iota'/2\pi$, ε_t, ε_h, ε_b, ε_{eff}, …) is a natural way to extract the key physics issues of developing the optimized helical-axis heliotron, where ε_t is the toroidicity defined as $\varepsilon_t = B_{10}/B_{00}$, ε_h is the helicity defined as $\varepsilon_h = B_{14}/B_{00}$, ε_b is the bumpiness defined as $\varepsilon_b = B_{04}/B_{00}$, ε_{eff} is the "effective helical ripple", where B_{mn} is the Fourier component of B in the Boozer coordinates. Global confinement studies have shown the beneficial role of $\iota/2\pi$ on global energy confinement time as indicated by the international stellarator scaling law such as ISS95 [5] and ISS04 [6]. As reported in Ref. [1], the experimental $\iota(a)/2\pi$ dependence of the enhancement factor of the global energy confinement time $H_{ISS95}(=\tau_E^{exp}/\tau_E^{ISS95})$ over the L-mode confinement has shown that the specific configurations exist where high-quality H-modes($1.3< H_{ISS95} <1.8$) are attained. The $\iota(a)/2\pi$ ranges for these configurations are near values that are slightly less than those of the major natural resonances of Heliotron J, i.e. n/m=4/8,4/7 and 12/22. With this in mind, as a next step of investigation, scans have been performed on Heliotron J with the bumpiness ε_b whilst the $\iota/2\pi$ value ($\iota(a)/2\pi=0.56$) was almost kept constant. Here the toroidicity ε_t, the helicity ε_h and the rotational transform $\iota/2\pi$ also remained almost fixed. Furthermore, the flexibility of Heliotron J operation allows the average magnetic axis position almost fixed for the central heating of ECH under the similar plasma volume conditions.

It is thought that the use of L-mode plasmas should help minimize the influence the edge features on global confinement, allowing a more direct study of the genuine influence of the bumpiness ε_b (or the "effective helical ripple", ε_{eff}) on core energy transport. A better understanding of the L-mode transport dependence on ε_b (or ε_{eff}) may open ways of improving the confinement quality of H-mode. ECH plasma is considered to be well suited to study the ε_b (or ε_{eff}) control dependence of τ_E^{exp} in Heliotron J since it can avoid the complications of beam ion orbit loss.

2. Experimental Set-up

Heliotron J is a medium-sized helical-axis heliotron device with major radius R=1.2 m, average plasma minor radius a = 0.1-0.2 m and magnetic field strength on its magnetic axis B_0 <1.5 T [7]. Its coil set can provide flexibility toward the configuration control of a helical-axis heliotron plasma [8]. The basic configuration of Heliotron J is achieved by the helical field coil, the two types of eight toroidal field coils and the main vertical field coil. The helical field coil is wound on the torus with the coil winding law of $\theta = \pi + (M/L)\phi - \alpha \sin \{(M/L)\phi\}$, where θ and ϕ are the poloidal and toroidal angles, respectively; M and L are the pitch number and the pole number of the helical coil, respectively, and are given in Heliotron J as M=4 and L=1; α is the pitch modulation factor of the helical coil and is given as α= -0.4. This highly negative α was chosen to ensure both the good particle confinement and the edge magnetic well. For the configurations with negative α, the major part of the deeply trapped particles are expected to be located at the straight section of the confinement region in which the ∇B drift of trapped particles is reduced. The radial build-up of the bumpy component in the Boozer coordinates in Heliotron J is also expected to play another important role in the confinement improvement, which produces a poloidal ∇B drift that improves the confinement of trapped particles. In addition, it is expected that even a small radial electric field improves the collisionless orbit confinement of bulk particles since the ∇B drift at the straight section is slow. The two types of eight toroidal field coils, located successively in the toroidal direction with different coil currents, can change the degree of the relevant bumpiness.

The details of ECH system are described in Ref. [9]. The injected power is up to 0.4 MW, and the pulse length is up to 0.1 s in the experiment. The Gaussian beam diameter of the second harmonic X-mode is 120 mm at the magnetic axis, which is about half of the plasma diameter on the equatorial plane. The ECH power absorption efficiency was estimated by using TRECE code [10] while taking into account the assumed 30% multireflection effects. As for the details of ICRF/NBI system, see Ref. [2, 13]. The diagnostics such as microwave interferometer, diamagnetic loop, visible light monitor, H_α/D_α emission detector, AXUV diode, Langmuir probes located in SOL, soft X-ray detectors, ECE monitors and so on are used to study the confinement characteristics of the plasma.

3. Experimental Results and Discussion

AS for the edge ι(a)/2π control, MHD properties also vary with the change of the ι(a)/2π value [11]. The close approach of the ι(a)/2π value to the major natural resonances was susceptible to MHD activity. For ι(a)/2π~0.49, the amplitudes of the magnetic fluctuation of m/n=2/1 with the frequency~15 kHz were observed to increase when the plasma current increased beyond the threshold current of about 2 kA, suggesting the appearance of ι/2π=1/2 inside the plasma. In this case, no drastic degradation of confinement was observed while the fluctuation amplitude increased with an increase in <β> up to 0.5%. The experiment showed the excitation of m/n=5/3 near the ι(a)/2π~0.6 and other numerous (unknown) modes with a change of ι(a)/2π, however, the detailed properties are now under investigation.

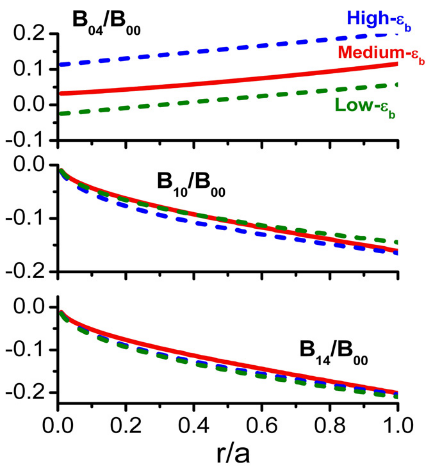

FIG.1 Bumpiness (B_{04}/B_{00}), toroidicity (B_{10}/B_{00}) and helicity(B_{14}/B_{00}) as a function of radius (r/a).

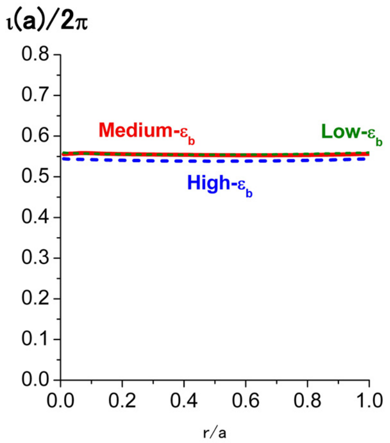

FIG.2 Rotational transform ι/2π for the high-ε_b, medium-ε_b, and low-ε_b configurations as a function of radius (r/a).

In addition to the edge ι(a)/2π control, the bumpiness control in Heliotron J is essential since the role of bumpiness is, as a feature of its conceptual design, to align the mod-B_{min} contours with the magnetic flux surfaces. In Heliotron E (helical heliotron), it was hard to ensure the compatibility between the drift optimization based on the inward magnetic-axis shift and the global magnetic well. On the other hand, Heliotron J (helical-axis heliotron) has a larger degree of flexibility that enables us to ensure this compatibility by using the bumpiness control which is achieved independently of the magnetic axis shift. As shown in Ref. [12] with model magnetic field and particle orbit calculations, the existence of closed mod-B_{min} contours necessitates a certain range of $\varepsilon_b/\varepsilon_h$, depending on the B_{min} value or the particle energy. The value of $\varepsilon_b/\varepsilon_h$ must be more negative as the ratio of $\varepsilon_t/\varepsilon_h$ increases, thus allowing to align the bottom of the magnetic field ripple. In order to extract the key physics ingredient linked with drift optimization for the improvement of the core and/or edge transport in L- and H-modes, three magnetic configurations were studied: (1) ε_b=0.01 (low bumpy), (2) ε_b=0.06 (medium bumpy), and (3) ε_b=0.15 (high bumpy) under the basically similar average magnetic axis position (R_{ax}), average minor radius (a), edge rotational transform (ι(a)/2π) conditions, where the bumpiness was chosen at the 2a/3 radius ε_b = $B_{04}(2a/3)/B_{00}(2a/3)$. See Figs. 1 and 2. The coil currents for the toroidal coils at the corner section (TA) and those in the straight section (TB) have been controlled independently: (1) for low bumpy, the current ratio is TA/TB=5/3, (2) for medium bumpy, TA/TB=5/2 and (3) for high bumpy, TA/TB=5/1. As shown in Fig. 3 in the medium-ε_b case, depending on the density evolution, ECH plasma gradually develops into H-mode at densities higher than the threshold density, followed by radiation collapse in a time scale of τ_E^{exp}. The change of

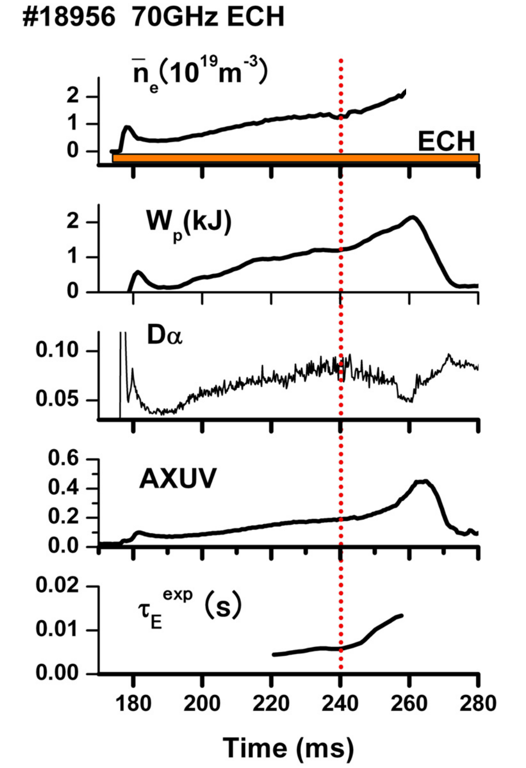

FIG.3 Time evolutions of the medium-ε_b ECH plasma parameters.

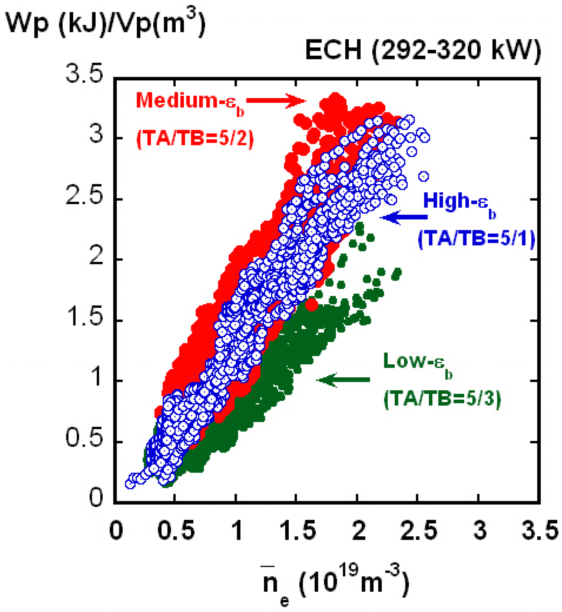

FIG. 4 Volume normalized plasma energy as a function of density for high-ε_b, medium-ε_b and low-ε_b ECH plasmas under the almost constant ECH power.

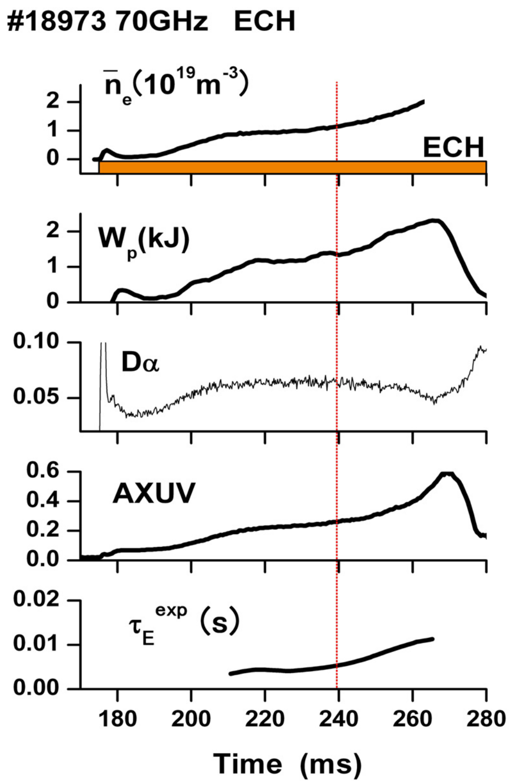

FIG. 5 Time evolutions of the high-ε_b ECH plasma parameters.

bumpiness is found to affect the detailed nature of H-mode transition and the resulting confinement quality. Figure 4 shows the volume normalized plasma energy attained as a function of density, suggesting that the medium-ε_b plasmas show better confinement than those of the high-ε_b and low-ε_b plasmas. For high-ε_b plasma as shown in Fig. 5, only a weak (or slow) L-H transition was observed at this ECH power level. This indicates that the configuration modified with the bumpiness affects the threshold nature of H-mode. For low-ε_b plasma as shown in Fig.6, the dithering transitions showed only a modest improvement of plasma energy content Wp as a result of density rise. With regard to the L-H transition, the neoclassical poloidal viscous damping rate coefficients $Cp=\langle(\mathbf{e}_p \cdot \nabla B/B)^2\rangle$ as a function of radius in the collisional regime which is relevant to the L-H transition in ECH plasmas are shown in Fig.7. Since the differences in Cp between the three configurations considered here are almost negligible, much more work will be necessary before comparison of the calculated poloidal viscous damping rate coefficient (Cp) with the L-H transition characteristics of Heliotron J in a similar way as in the case of the edge iota control studies [1].

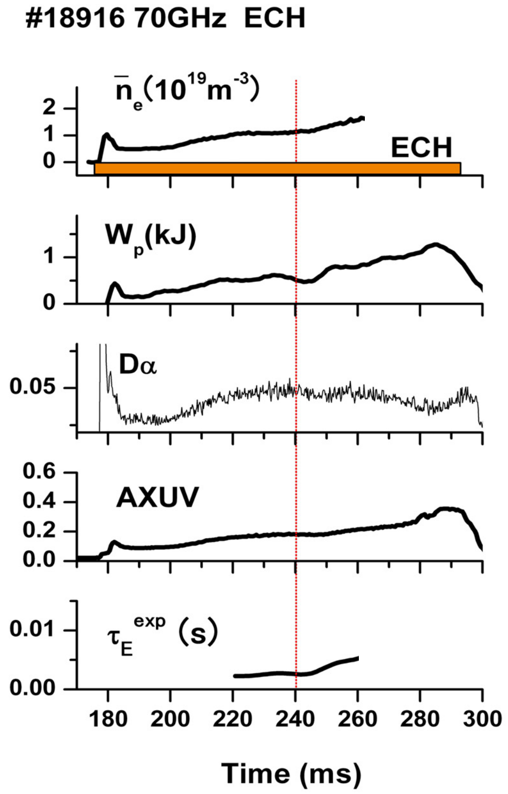

FIG. 6 Time evolutions of the low-ε_b ECH plasma parameters.

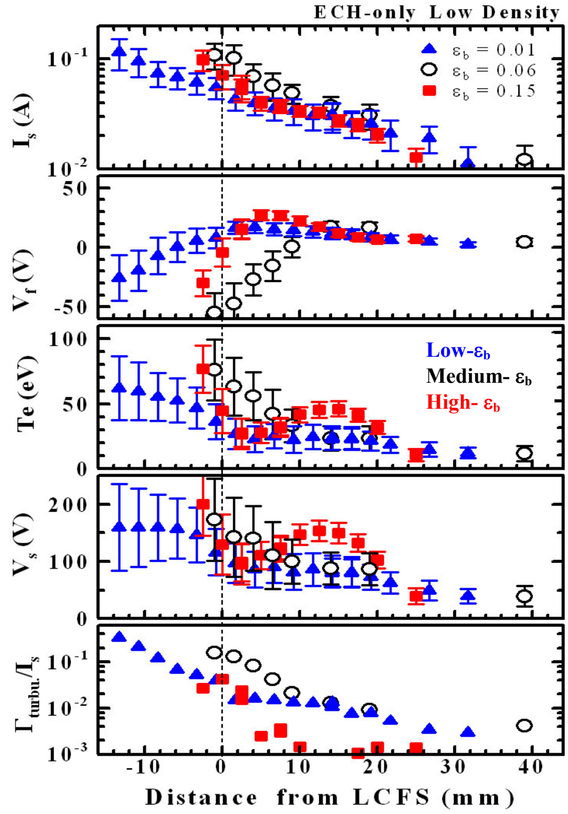

FIG.8 Edge and SOL plasma parameters as a function of the distance from the LCFS for ECH-only low density plasma.

In connection with the bulk plasma confinement, the edge and SOL plasma properties were investigated. As shown in Fig. 8, in low-density ECH plasma of $\bar{n}_e = 0.4 \times 10^{19} m^{-3}$, measurements of the distributions of (i) the ion saturation current I_s, (ii) the floating potential V_f, (iii) the electron temperature Te, (iv) the estimated space potential $V_s(=V_p+3Te)$, and (v) the turbulence-induced particle flux $\Gamma_{turbu.}$ normalized by I_s near the last closed flux surface (LCFS) by a movable Langmuir probe showed a characteristic feature of some edge and SOL parameters in the medium-ε_b case. The inflection point of V_f-profile is observed to be located a longer way from the LCFS in the medium-ε_b case. Inside this inflection point (d=12 mm), both of Is, Te, Vs and $\Gamma_{turbu.}/I_s$ are higher than in other cases while V_f is much lower. The steeper gradient in Te (and Is, V_f, Vs) at the LCFS is observed with an increase in bumpiness ε_b. Another important feature is the significantly lower Te and Is distributions inside the LCFS in the low-ε_b case. These findings may be the important circumstantial evidence to relate the degradation of neoclassical drift optimization in the low-ε_b case with an enhanced anomalous edge transport.

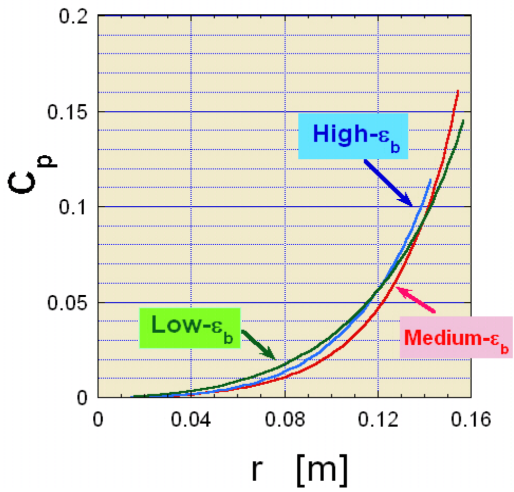

FIG. 7 Calculated neoclassical poloidal viscous damping rate coefficient C_p as a function of radius r (m) for high-ε_b, medium-ε_b and low-ε_b configurations.

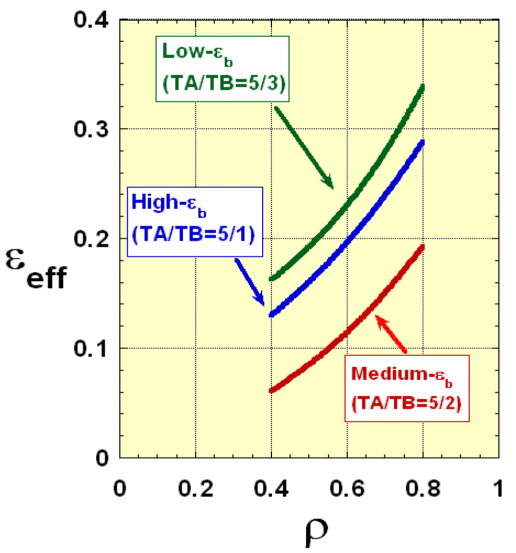

FIG. 9 Calculated "effective" helical ripple ε_{eff} as a function of radius for high-ε_b, medium-ε_b and low-ε_b configurations.

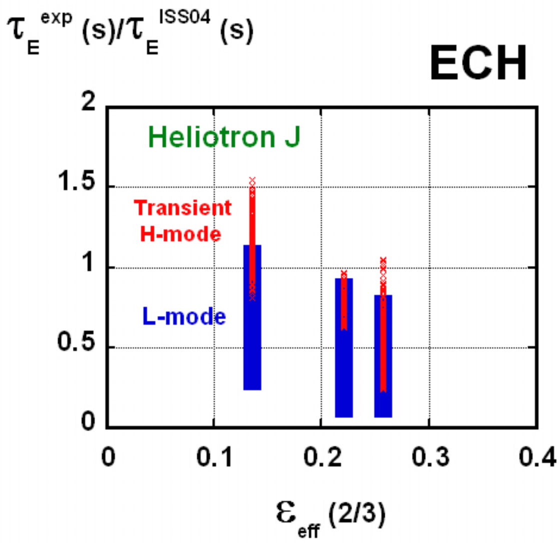

FIG. 10 Confinement enhancement factor, H_{ISS04}, with regard to the ISS04 scaling as a function of ε_{eff} at r/a=2/3 for ECH plasmas with the bumpiness modified configurations.

As for the bulk plasma confinement, the reduction of the neoclassical transport depends on the appropriate choice of ε_b [8]. Here, the "effective helical ripple", ε_{eff}, in the 1/ν collisionless regime was calculated by the Monte Carlo technique for the three configurations considered here. The results[1)] from the DCOM code showed that the medium-ε_b configuration provides a greater degree of neoclassical optimization in the 1/ν collisionless regime as shown in Fig. 9. Figure 10 shows the relationship between the ratio of the global energy confinement time τ_E^{exp} to the international stellarator scaling law (τ_E^{ISS04}) and the calculated "effective helical ripple", ε_{eff} , at r/a=2/3 for 0.3-MW, 70-GHz on-axis ECH plasmas, where R_{ax}~1.20 m, $\iota/2\pi(a)$~0.56 are nearly kept the same and $\tau_E^{exp}=W_p/(P_{abs}-dW_p/dt)$; W_p is the diamagnetic plasma energy; P_{abs} is the ECH absorption power estimated using TRECE code under the condition of single-pass absorption modified by the assumed 30%

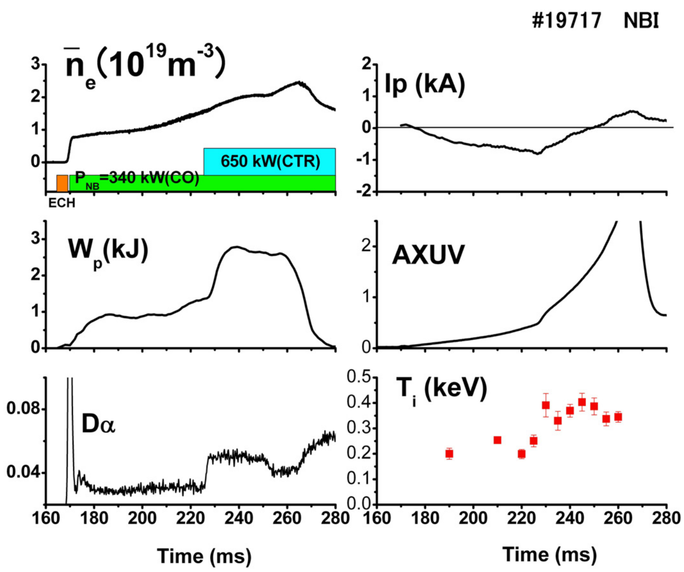

FIG.11 Time evolutions of plasma parameters in the stage-injection of NBI (CO and CO+CTR) in the medium-ε_b configuration.

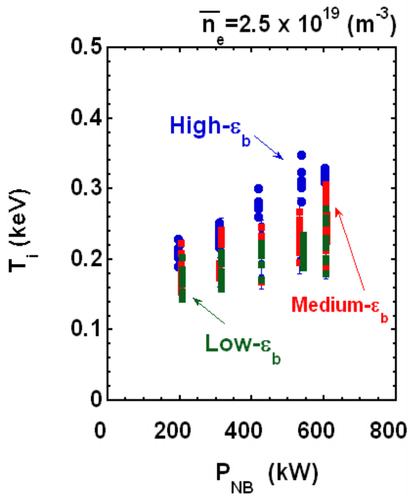

FIG.12 Ion temperature increase as a function of NBI injection power under the constant density of $\bar{n}_e$=2.5 x 10^{19} m^{-3} for the high- ε_b, medium-ε_b and low-ε_b configurations..

[1)] The results (ε_{eff}) were recently revised and a factor of two larger than before.

multi-reflection effects. It may be suggested that the reduction of ε_{eff} introduces a favourable effect on the confinement of ECH in the L- and the transient H-mode phases. However, due to the large data scatter and inherent error bars, further studies are necessary to understand the more statistical and physical trends of anomalous confinement by accumulating the sufficient data and by measuring the turbulence structure including the plasma electric field, plasma flow, etc.

As a final observation, it should be commented here that the experimental comparison between the bumpiness dependence of thermal confinement and that of energetic ion confinement produces a question. As for NBI heating, an example of plasma parameters in the stage-injection mode of NBI is shown in Fig.11. In this case, the target deuterium plasma for NBI(H^0) was produced only by short-pulse ECH, and then NBI-only plasma was sustained in the stage-injection mode, where NBI injection power (P_{NB}) in the 1st stage is 340 kW(CO) and that in the 2nd stage is 990 kW(CO+CTR). In the 2nd stage, the ion temperature measured with the neutral particle analyzer (NPA) reaches about 0.4 keV at $\bar{n}_e = 2 \times 10^{19} m^{-3}$. In order to avoid the complicated NBI heating situations for the configuration control studies, the increase of ion temperature only for the CO injection mode was measured by changing the bumpiness under the conditions of the constant density of $\bar{n}_e = 2.5 \times 10^{19} m^{-3}$, as shown in Fig. 12. The results suggest that the high-ε_b configuration provides better ion heating efficiency as compared with that of the medium-ε_b or low-ε_b configuration. At these densities, the shine-through loss of beam ions is predicted to be on the order of 10-30% of injection power, depending on the injection angle of each ion source of the beam line. The ion orbit loss and charge-exchange loss depend on the bumpiness; the Helios code results predict a relatively high loss rate, however, the detailed estimations of the change of NBI absorption power with the change of bumpiness still remain as a future work due to the complications of ion orbit loss. On the other hand, as shown in Ref. [13], measurements of the charge-exchange (CX) neutral particle flux (at the toroidal angle 12 degree of the neutral particle analyzer NPA that views the passing orbits) just after the neutral beam (NB) turn-off have revealed that the CX-flux decay time improves with an increase in bumpiness, indicating the effective confinement improvement of helically trapped or toroidally trapped fast ions in the high-ε_b case. By using ICRF minority (H) heating to the ECH target plasma (D), the formation and confinement of high energy ions were studied with special regard to the bumpiness modification under almost the same central resonance conditions by adjusting the ICRF frequency. From the experiments, it was suggested that the tail ion temperature increases with an increase in bumpiness ε_b under the same density ($\bar{n}_e = 0.4 \times 10^{19} m^{-3}$) and RF injection power (200 kW) conditions [2].

Therefore, to determine what effect in the global energy confinement – ignored here, e.g. electric field, turbulent plasma flow shear, etc. - makes up this apparent difference would shed an interesting light on the different properties of thermal and energetic ion confinement in the helical-axis heliotron.

4. Summary

Heliotron J experiments have progressed toward its research mission of the concept exploration of an optimized helical-axis heliotron. The main experimental results are concerned with thermal confinement, fast ion confinement, MHD, plasma current control, edge/SOL plasma properties and divertor plasma dynamics. Magnetic configuration control studies were performed with special regard to vacuum edge iota control and bumpiness control for low-β plasma confinement. With regard to edge iota control [1], L-H transition characteristics have been studied on the basis of their threshold (or boundary) conditions of density, power, plasma-wall interactions, etc. However, the observed H-mode still remains transient in a time scale of τ_E while the steady-state phase is not yet achieved. The experimental efforts toward this direction is necessary. Bumpiness control studies have clarified the important role of bumpiness in the effective control of plasma current [3], fast ion confinement [2], bulk plasma confinement and edge/SOL plasma characteristics. From the measurements of bulk plasma energy confinement of ECH plasmas, it may be suggested that the lower ε_{eff} configuration provides better thermal confinement. On the other hand, as for fast ion confinement in NBI and ICRF heating, the experiment suggests that the higher bumpy configuration provides more favourable fast ion confinement than that of the medium or low bumpy configuration studied here. Further studies are necessary to determine what effect (including the plasma flow and/or edge/SOL plasma behaviour) makes up this difference of "effective helical ripple" (ε_{eff}) dependence or bumpiness dependence between thermal confinement and fast ion confinement. This is an important task that should be continued in the Heliotron J experiments.

Acknowledgement

The authors wish to thank Dr. V. Tribaldos at CIEMAT, Dr. S. Murakami at Kyoto University and CHS/LHD teams at the National Institute for Fusion Science (NIFS) for their theoretical and experimental contributions and helpful discussions. This work is performed with the support and under the auspices of Kyoto University 21st century COE Program as well as the NIFS Collaborative Research Program (NIFS04KUHL005 and NIFS04KUHL001-010).

References

[1]SANO, F., et al.,20th IAEA Fusion Energy Conference, Vilamoura, Portugal, 1-6 November 2004, IAEA-CN-116/EX/9-2. SANO., F., et al., Nucl. Fusion **45**(2005)1557.
[2]OKADA, H., et al., *in this conference (EX/P6-1).*
[3]NAGASAKI, K., et al., *in this conference (EX/P6-14).*
[4]MIZUUCHI, T., et al., *in this conference (EX/P4-18).*
[5]STROTH, U., et al., Nucl. Fusion **36**(1996)1063.
[6]YAMADA, H., et al., Nucl. Fusion **45**(2005)1684.
[7]OBIKI,T., et al., Nucl. Fusion **41**(2001)833.
[8]WAKATANI, M., et al., Nucl. Fusion **40**(2000)569.
[9]SHIDARA, H., et al., Fusion Science and Technology, Vol. **45**, Jan. 2004, p.41.
[10]TRIBALDOS, V., et al., J. Plasma Fusion Res. **78**(2002)996.
[11]YAMAMOTO, S., et al., in 15th International Stellarator Workshop, Madrid, October 3-7, 2005, Paper P2-27.
[12]YOKOYAMA, M., et al., Nucl. Fusion **40**(2000)261.
[13]KOBAYASHI, S., et al., 20th IAEA Fusion Energy Conference, Vilamoura, Portugal, 1-6 November 2004, IAEA-CN-116/EX/P4-41.